Influence of Joint Configuration on Linear Friction Welded Ti-6Al-4V Alloy Joints

* **P. Hariprasath**, Research Scholar; [1]**Dr. P. Sivaraj**, Associate Professor
[2]**Dr. V.Balasubramanian**, Professor and Head
*,[1],[2]Centre for Materials Joining and Research (CEMAJOR)
Department of Manufacturing Engineering, Annamalai University
Annamalai Nagar -608002, Tamil Nadu, India
*Email: hariprasathp12mech@gmail.com
[3]**Dr.Vijay Petley**, Scientist F; [4] **Shweta Verma**, Scientist D
[3],[4]Materials Group, Gas Turbine Research Establishment (GTRE)
DRDO, Bengaluru, India

ORCID: P Hariprasath: https://orcid.org/0000-0003-1338-6339
ORCID: P Sivaraj: : https://orcid.org/0000-0002-3989-5484
ORCID: V. Balasubramanian: https://orcid.org/0000-0001-7658-6392
ORCID: Vijay Petley: https://orcid.org/0000-0003-0821-0929
ORCID: Shweta Verma: https://orcid.org/0000-0003-2789-8036

Abstract

Ti-6Al-4V alloy is a unique material for structural applications of aerospace industry for the excellent strength and lightweight. The fusion welding of this Titanium alloy resulted severe residual stress formation and coarser grains in the fusion zone. To overcome these problems, a solid state linear friction welding (LFW) is a emerge technique to joining of blade and disk assembly in the next generation aero engines. The plastic deformation followed by forging action resulted finer grain structures in welded regions. This investigation elaborated mechanical behavior and microstructural characteristics of linear friction welded joints. The welding parameters established by statistical response surface methodology. The fabricated joints yielded maximum tensile strength and joint efficiency of 1011 MPa and 98%. The lower microhardness recorded in the thermo mechanical affected zone (TMAZ) among the weld cross section. The weld nugget microstructure composed of equiaxed grain structure. The fracture surface revealed that joints failed under ductile mode. The result concluded that the weld failure mainly due to grain coarsening subsequent deformation leads to weld failure in the LFW joint.

Keywords: Linear friction welding; titanium alloy; microhardness; microstructures; fractography.

1.0 Introduction

Ti-6Al-4V [Ti-64] alloy is a unique super alloy consider for high strength to weight ratio, high-temperature sustainability, and anti corrosion behaviors suitable in defence, aerospace, nuclear and, petrochemical sectors. In particular, Ti-64 alloy is used in bladed and disk [blisk] assembly in aero engines [1-3]. Gas tungsten arc welding (GTAW) is a most common process for joining titanium alloys. But, the higher heat input results in greater distortion, and inclusion defects in weldment [4]. Radiant energy welding processes like a laser and electron beam welding processes also used for joining titanium alloys but the higher cooling rate possesses problems like porosity and fusion zone cracking [5]. Therefore, the researchers prefer solid-state techniques to join both similar and dissimilar aerospace alloys. Among these techniques, the friction welding offers many advantages like the elimination of consumables, less welding time, higher joint efficiency, etc.

Linear friction welding (LFW) is a variant of the friction welding process, where the joint between two materials is made by the relative motion and the compressive forces [6]. In LFW, one part is kept stationary and the other part is oscillating linearly. During this process, the frictional heat will be generated between the surfaces and the plasticized region forms at the interface. Then the symmetrical and asymmetrical flash formed at the end of applied force [7]. Abbasi et al. analyzed metallurgical characteristics of different filler metal composition on Ti-6Al-4V alloy joints. The weld metal micro-structure consists of both acicular and basketweave morphologies [8]. Babu et al. reported Pulsing current characteristics on GTA welded Titanium alloy joints. The pulsing effect improved strength and ductility by grain refinement of prior β phase [9]. Balasubramanian et al. investigated the corrosion behavior of pulse enhanced GTA welded Ti64 alloy. The corrosion resistance increased with increasing pulsing frequency and peak current and then get

decreased. The finer grains developed in the fusion zone will be responsible for the increased corrosion resistance [10]. Cao et al. reported that microstructure characteristics of laser welded Ti64 joints. It found that 20% martensite (α') increased in weld region compared with parent. The inhomogeneous micro-structure resulted reduction in tensile strength and lower ductility [11]. Romero et al. establish the forging pressure characteristcis on residual stress development of LFW joints. They concluded that the forging pressure has more influence on weld width and thermomechanically affected zone (TMAZ). During welding, the temperature developed at the weld region and TMAZ exceeds β transition temperature [12]. Li et al. reported that friction time influence on flash shape and upset of steel joints made by LFW process. They reported upset length increases linearly with increasing time. The flash formation is an undulating-ribbon structure in the direction of friction and curly edges in the vertical direction [13]. From the literature survey, limited investigation has been conducted on linear friction welding of titanium alloys. Also most of the published information on Titanium alloys are related to fusion welded joints. Therefore, the present work deals with linear friction welding joint configuration mechanical and microstructural characteristics of Ti-6Al-4V joints.

2.0   Materials and Methods

Ti-6Al-4V plates with 6 mm thickness was used for this investigation. **Tables 1 & 2** represents the relative elemental composition and mechanical properties of parent alloy. **Fig. 1 (a-b)** represents the base metal microstructure of titanium alloy, which consists of bimodal phases of α and β with different crystallinity structures such as hexagonal closed packing (HCP) structure and body-centered cubic (BCC) structure.

The welding experiment was carried out through Hydraulic enabled Linear friction welding (LFW) machine (Make: RV machine tools). As shown in **Fig. 2(a-b)** represented blisk assembly and working mechanism of Linear friction welding process. The most influencing process parameters are: Friction
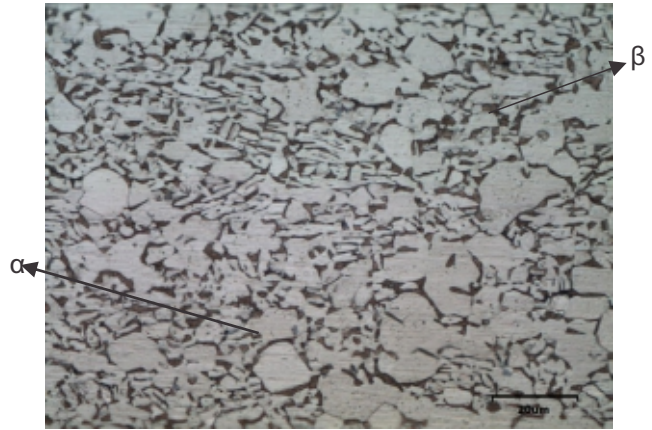
(a) Optical micrograph of Ti64 alloy
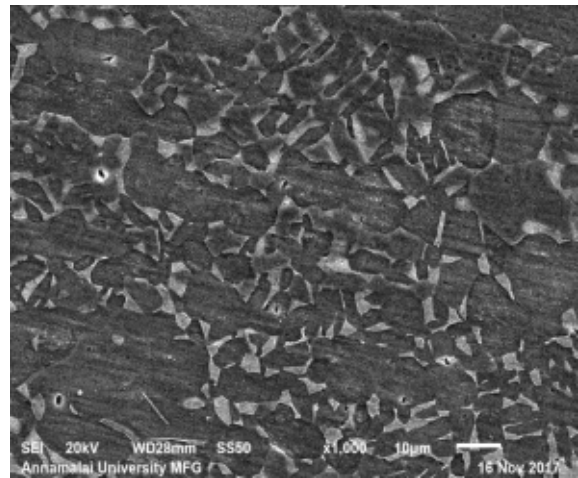
(b) SEM image of Ti64 alloy

Fig. 1 : Micrographs of Ti64 alloy

Table 1 : Elemental constituents (wt%) in Parent alloy

Elements	Al	V	Fe	O	C	N	H	Ti
Ti-6Al-4V	6	4	0.18	0.16	0.061	0.039	0.01	Bal.

Table 2 : Parent alloy Mechanical properties

0.2 % Yield Strength (MPa)	Ultimate Tensile Strength (MPa)	Elongation (%)	Vickers hardness, (HV0.05)	Impact Toughness @ RT (J)
980	1030	12	439	26

Pressure (FRP), Friction Time (FRT), Forging Pressure (FOP), Forging Time (FOT), and Oscillating Frequency (OF). **Table 3** represented the suitable working limit for defect-free joints obtained from trial experiments. **Table 4** exhibited the optimized LFW process parameters for welding Titanium alloy obtained with aid of response surface methodology (RSM).

The tensile test has performed on defect-free joints using a hydraulic enabled UTM with constant strain rate. **Fig.2** displays the fabrication details of LFW joints and tensile specimen. And, Vicker's microhardness tester was used to measure the hardness across weld cross section with 50 g load and 15 sec dwell time (Make: SHIMADZU). To examine metallurgical features acrkss the weld cross-section, a stereo zoom macroscope (Make: Zeiss) and optical microscope (Make: Nikon climax) were used to characterize the defect-free LFW joints. The Kroll's reagent (100 ml H_2O + 2 ml HF + 5 ml HNO_3) was applied to reveal the microstructural features. The failure surfaces were characterized with help of scanning electron microscopy (SEM) and elemental analysis done by electron diffraction spectroscopy (EDS) (Make: JEOL).
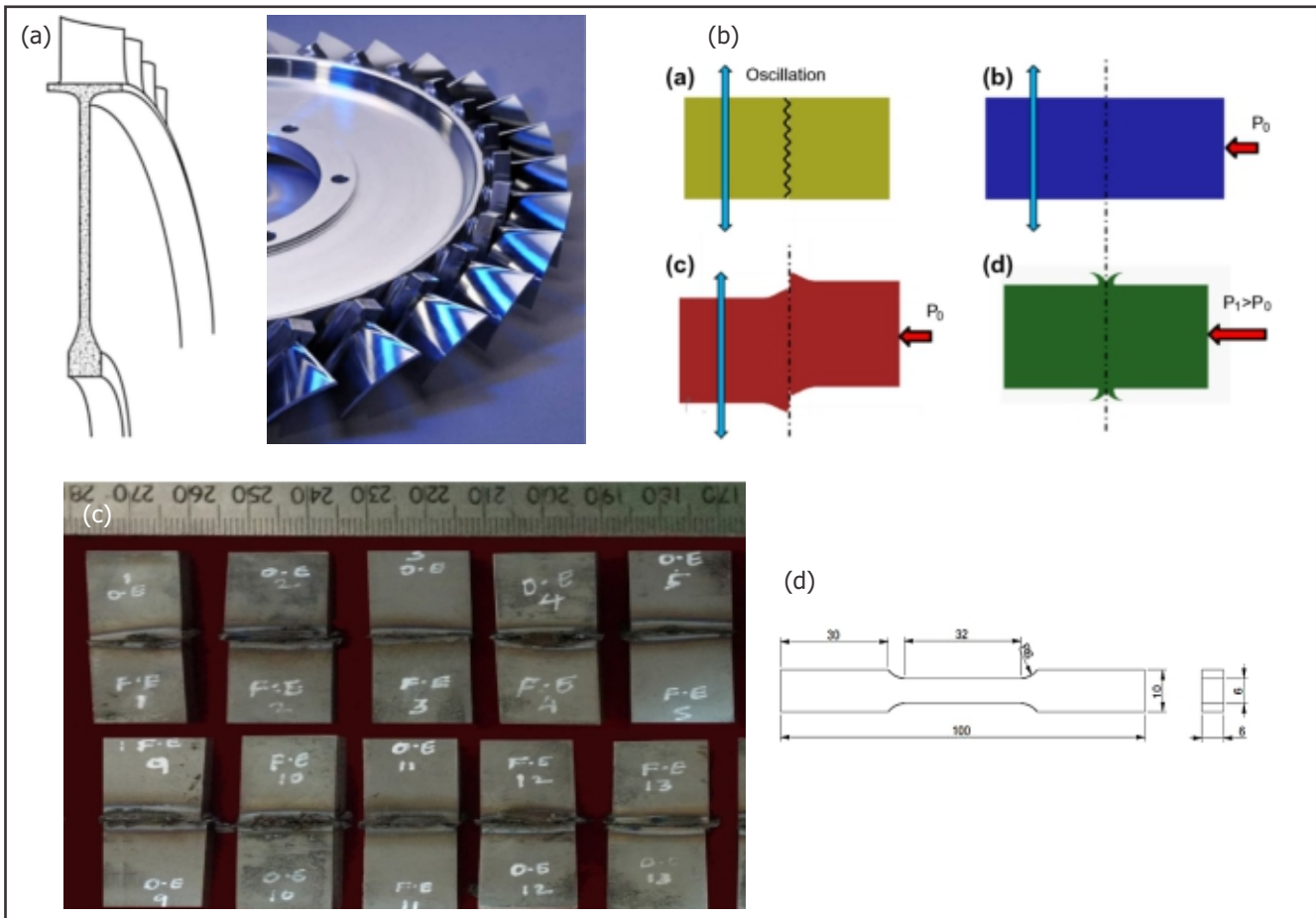

Fig. 2 : (a). blisk assembly set up; (b). working mechanism of Linear friction welding;
(c). Fabricated joints; (d). tensile specimen configuration

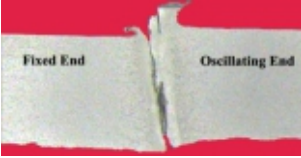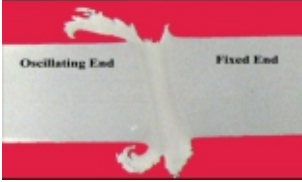Table 3 : Identifying feasible working limit of fabricated joint

Parameters		Photograph	Macrograph	Observation
OF FRP FOP FRT FOT	<11 Hz <12 MPa <11 MPa <15 sec =3 sec		------	Not welded
OF FRP FOP FRT FOT	<13 Hz <11 MPa <3 MPa <25 sec =2 sec			Welded with macro level defect
OF FRP FOP FRT FOT	>14 MPa >25 sec >3 MPa =2 sec >15 Hz			Welded with non-uniform flash formation
OF FRP FOP FRT FOT	<22 MPa =40 sec <11 MPa =3 sec >17 Hz			Welded with the good flash formation on both sides
OF FRP FOP FRT FOT	>27 MPa >35 sec <11 MPa =3 sec >19 Hz			Welded with macro level defect

Table 4 : Optimized welding parameters used to fabricate the joints

Parameter	LFW
Oscillating frequency (Hz)	17
Forging pressure (MPa)	11
Forging time (sec)	6
Friction pressure (MPa)	22
Friction time (sec)	40

## 3.0 Results

3.1 Tensile Behavior

The tensile test has conducted for analyzing elastic to plastic deformation changes and the load-carrying capacity of the LFW joint. The maximum obtained yield strength of 926 MPa, ultimate tensile strength of 1011 MPa and uniform elongation of 7.5 % and with joint efficiency of 98% was obtained, it showed in **Table 5**.

The weld failure observed in the fixed end of thermomechanical affected zone (TMAZ). The weld failure mainly due to grain coarsening of α phase and subsequent deformation. The severe deformation at the weld interface leads to lower ductility than the base metal. **Fig. 3** represented before and after tensile test specimens. According to Fratini et al. reduction in strength and failure occurred mainly due to dissolution or segregation precipitates [14] .

Table 5 : Tensile properties for optimized parameters

0.2% Yield strength (MPa)	Ultimate Tensile strength (MPa)	Uniform elongation (%)	Joint efficiency (%)	Fracture region
926	1011	7.5	98	TMAZ
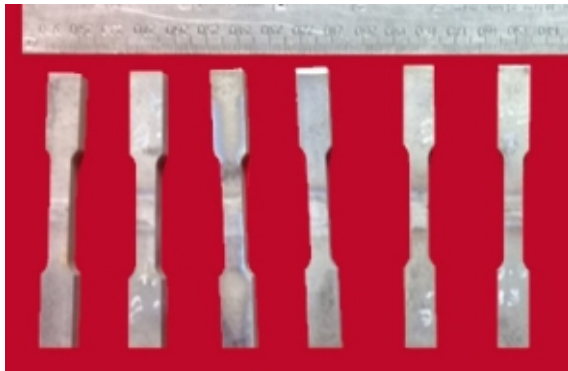
(a) Before testing   (b) After testing

Fig. 3 : Photograph of tensile specimen

3.2 Microhardness Variations Across the Joints

The microhardness measurement helps to analyze the hardness variation along the cross-section. **Fig. 4** illustrates the hardness map of LFW joint across the weld cross-section. Chamanfar et al. reported that microhardness is sensitive to reflect small microstructural changes during plastic deformation and solidification [15]. The maximum recorded hardness value of 389±10 HV due to the formation of recrystallization grains at the weld interface. The microhardness steeply dropped in the thermomechanical affected zone (TMAZ) about 310±5 HV. The combined action of frictional heat and forging pressure resulted in elongated coarse grains at the TMAZ region, so the hardness is slightly decreased in this region [16]. The heat-affected region (HAZ) lower deformed region compared with the TMAZ region. Therefore, the HAZ region recorded a hardness value of 330±5 HV.

3.3 Macro and Microstructural Features of the LFW Joint

The macrograph was used to analyze the joint quality and weld integrity of the LFW joint and it is shown in **Table 3**. At lower range parameters frictional heat was not enough to plasticize the material. At higher level welding parameters more diffusion occurred at the interface which led to inclusion defects. In optimized condition defect-free and asymmetric flash formed

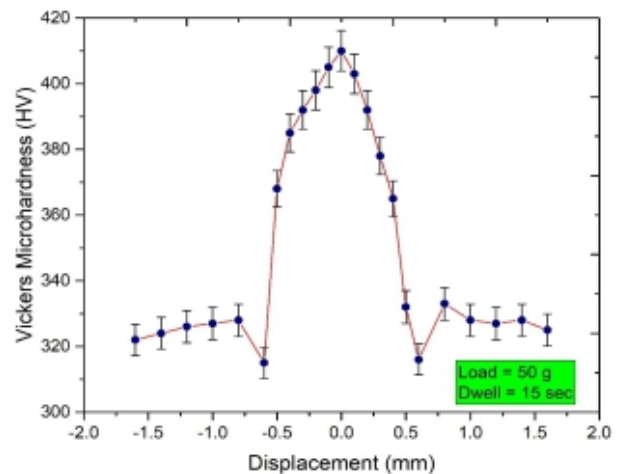Fracture occurred at PDZ / HAZ interface

Fig. 4 : Microhardness variation across the LFW joint

at both side of Ti64 alloy joint and it showed in **Fig.5**. **Fig. 5a** represents the fully deformed microstructure of the weld center, which composed of fine equiaxed grain structure. The dynamic recrystallization grains exhibited α and β phases along with needle-like martensite (ȧ) and widmanstantten (basket-weave) structure. According to Ji et al. the recrystallized grain structure formed due to applied mechanical force at the end of the deceleration section [17]. As shown in **Fig 5b**, the dark field SEM microstructure illustrates the presence of needle-like martensites at the weld center (NZ). During plastic deformation bimodal α–β phases transformed into widman-stantten α phase and prior β grain boundaries mutate to martensite (ȧ) structure as discussed by Xinyu Wang et al [18]. **Fig. 5 (c-d)** represents the TMAZ of oscillating and fixed end region, it observes metal flow and grain deformation. This is narrow region compared to NZ and it is formed due to the combined action of frictional heat and forging pressure. Also, the microstructure of HAZ having lower plastic deformation compared with TMAZ and it is shown in **Fig. 5 (e-f)**.
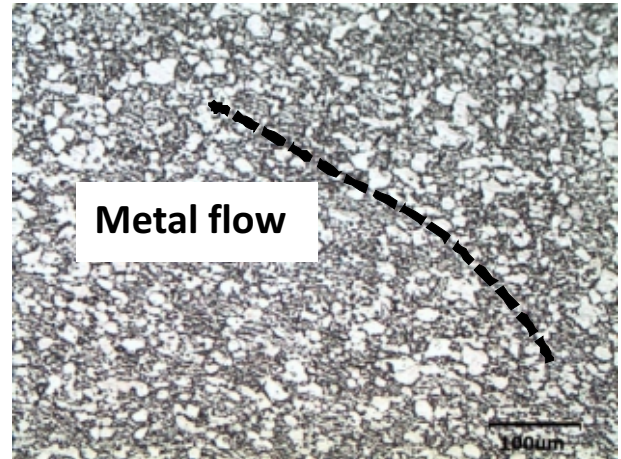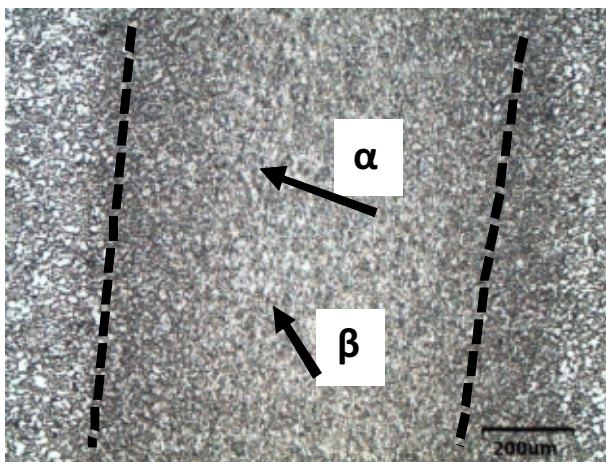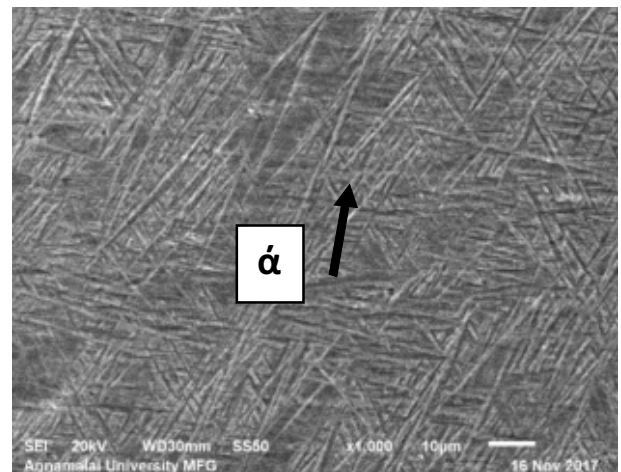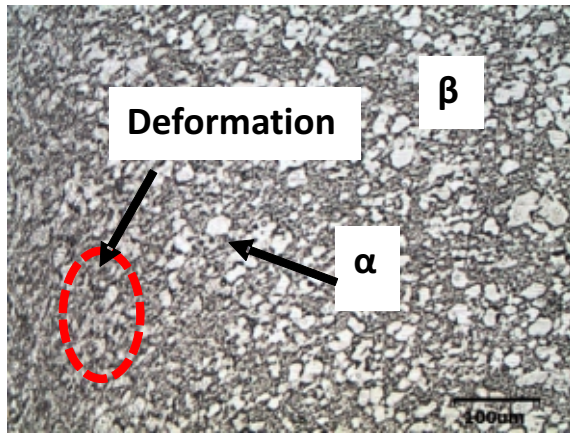

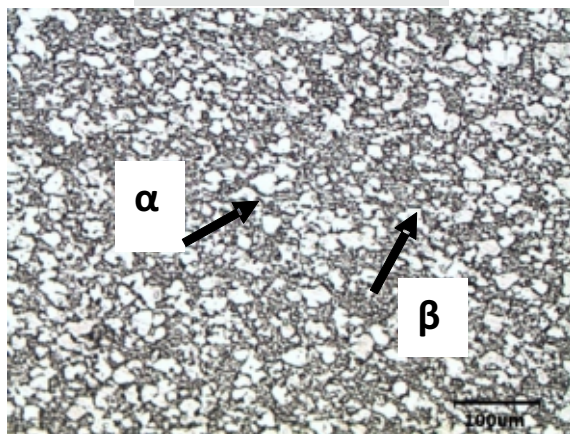(b) TMAZ Osilatation end
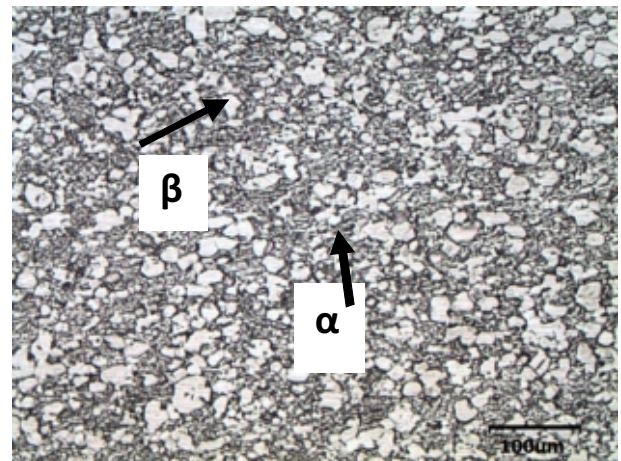
(c) HAZ Osilatation end
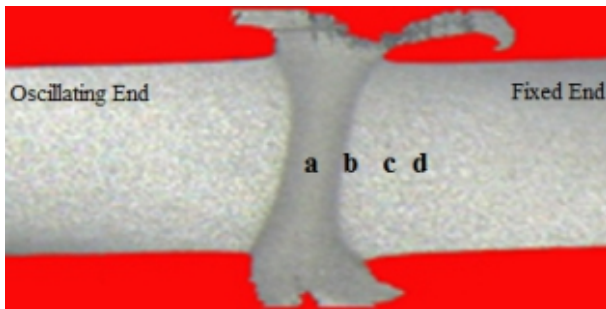
I. Macrostructure

(a) WNZ

(d) WNZ

(e) TMAZ fixed end

(f) HAZ fixed end

Fig. 5 : Macro and Microstructural features of LFW joints

(a) Low magnifaication

(b) Dimple features

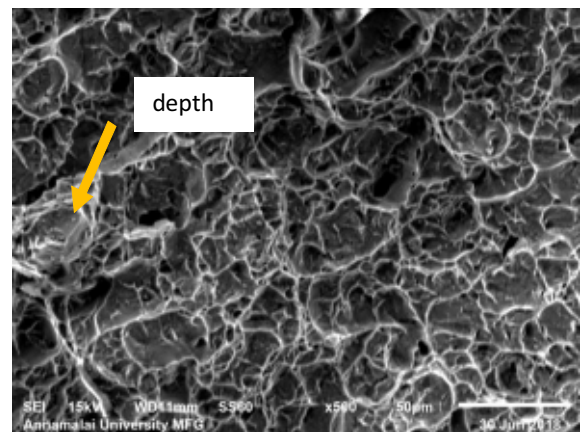(c) Dimple features

3.4 Fractography

The fractogaphy reveal the mode of failure on the LFW joint. The weld failure initiated and propagated through the TMAZ region, due to severe deformation and lower microhardness. As shown in **Fig. 6a**, the semi quasi cleavage fracture occurred in the LFW joint. The lower microhardness attributed to this failure. **Fig. 6 (b-c)** revealed fine dimple features in the propagated region in the fractured specimen, whereas dimple features ensured the ductility of LFW joint. The strength and hardness superior in finer dimples compared to coarser [19].
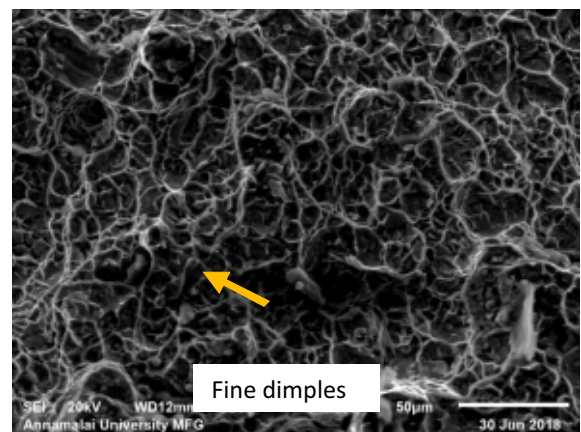
4.0 Discussion

The solid-state LFW process produces several advantages rather than fusion welding processes. The derived tensile properties ensure ensure that 98% equals to the base metal. The elastic straining followed by deformation assist the weld failure in LFW joints. The differential cooling rates attributed to higher microhardness in the Nugget zone (NZ). In most of the

Fig. 6 : Fracture surfaces of tensile specimens

cases weld center recorded higher hardness, although similar hardness variation observed in LFW joints [20,21]. It mainly due to phase transformation and ultra-refined grain structure in the nugget zone (NZ) [22]. The failure initiates from the TMAZ region, it is found to beweakest region among the weld cross-section. Also, the superior tensile and hardness properties attributed by refinement of grains. The nugget microstructure details the phase transformation morphologies of LFW joints. The bimodal microstructure of alpha (α) and beta (β) grains in the base metal is transformed into the Widmanstädtern (basketweave) and needle-like martensite (ὰ) structure.The following phase changes occurred in the microstructure such as $α \rightarrow β \rightarrow α$ (Widmanstädtern) + martensite (ὰ) phase during weld thermal cycle. Dong He et al. evident that phase transferred refined prior-β grains in the fully deformed region (FDZ) at weld center [23]. The beta transition temperature at 995 °C in the Ti64 alloy, whereas except weld center there is no phase transformation occurred in the other regions [24,25]. The heterogeneous microstructure of TMAZ region attributed to weld failure. The finer dimple patterns observed from the fractured surface, which confirms that ductile features in the Ti64 alloy joint.

4.0 Conclusions

The important conclusions derived from this investigation:

i. The maximum observed yield and tensile strength of LFW joints are 926 MPa and 1011 MPa; it is 98 % equal to unwelded base metal strength.

ii. The hardness is inhomogeneous across the LFW joint and the lowest hardness value is recorded at the TMAZ region, where the failure initiated and propagated.

iii. In LFW joints, the failure occurred at the TMAZ region due to the grain coarsening and subsequent softening.

iv. The microstructural analysis reveals the formation of Widmanstädtern (α) and martensite (ὰ) structure at the weld nugget zone and reoriented and elongated bimodal alpha and beta grains in the TMAZ region.

v. The ductile mode of failure is observed in the joints and it is confirmed with finer dimple pattrens in the fracture surface.

Acknowledgments

References

[1] Bhamji I, Preuss M, Moat RJ, Threadgill PL and Addison AC (2012); Linear friction welding of aluminium to magnesium. Sci Technol Weld Join., 17 (5), pp. 368-374 .

[2] Gao XL, Zhang LJ, Liu J and Zhang JX (2013); A comparative study of pulsed Nd: YAG laser welding and TIG welding of thin Ti6Al4V titanium alloy plate. Mater Sci Eng A., 559, pp. 14-21.

[3] McAndrew AR, Colegrove PA, Bühr C, Flipo BCD and Vairis A (2018); A literature review of Ti-6Al-4V linear friction welding. Prog Mater Sci., 92,pp.225-257.

[4] Guo Y, Attallah MM, Chiu Y, Li H, Bray S and Bowen P (2017); Spatial variation of microtexture in linear friction welded Ti-6A-4V. Mater Charact., 127, pp.342-347.

[5] Fall A, Jahazi M, Khdabandeh AR and Fesharaki MH (2017); Effect of process parameters on microstructure and mechanical properties of friction stir-welded ti-6al-4v joints. Int J Adv Manuf Technol., 91, pp. 2919-2931.

[6] Wanjara P and Jahazi M (2005); Linear friction welding of Ti-6Al-4V: Processing, microstructure, and mechanical-property inter-relationships. Metall Mater Trans A Phys Metall Mater Sci., 36, pp2149-2164.

[7] Meschut G, Janzen V and Olfermann T (2014); Innovative and highly productive joining technologies for multi-material lightweight car body structures. J. of Materi Eng and Perform., 23, pp.1515-1523.

[8] Abbasi K, Beidokhti B and Sajjadi SA (2017); Microstructure and mechanical properties of Ti-6Al-4V welds using α, near-α and α+β filler alloys. Mater Sci Eng A., 702, pp.272-278.

[9] Kishore Babu N, Ganesh Sundara Raman S, Mythili R and Saroja S (2007); Correlation of microstructure with mechanical properties of TIG weldments of Ti-6Al-4V made with and without current pulsing. Mater Charact., 58, pp.581-587.

[10] Balasubramanian M, Jayabalan V and Balasubramanian V (2008); Effect of pulsed gas tungsten arc welding on corrosion behavior of Ti-6Al-4V titanium alloy. Mater Des., 29, pp. 1359-1363.

[11] Cao X and Jahazi M (2009); Effect of welding speed on butt joint quality of Ti-6Al-4V alloy welded using a high-power Nd:YAG laser. Opt Lasers Eng., 47, pp. 1231-1241.

[12] Romero J, Attallah MM, Preuss M, Karadge M and Bray SE (2009); Effect of the forging pressure on the microstructure and residual stress development in Ti-6Al-4V linear friction welds. Acta Mater., 57, pp. 5582-5592.

[13] Li WY, Ma TJ, Yang SQ, Xu QZ, Zhang Y, Li JL and Liao HL (2008); Effect of friction time on flash shape and axial shortening of linear friction welded 45 steel. Mater Lett., 62, pp. 293-296.

[14] Fratini L, Buffa G, Cammalleri M and Campanella D (2013); On the linear friction welding process of aluminum alloys: Experimental insights through process monitoring. CIRP Ann - Manuf Technol., 62, pp. 295-298.

[15] Chamanfar A, Jahazi M, Gholipour J, Wanjara P and Yue S (2011); Mechanical property and microstructure of linear friction welded WASPALOY. Metall Mater Trans A Phys Metall Mater Sci., 42, pp.729-744.

[16] Hua K, Xue X, Kou H, Fan J, Tang B and Li J (2014); Characterization of hot deformation microstructure of a near beta titanium alloy Ti-5553. J Alloys Compd., 615, pp. 531-537.

[17] Ji Y, Chai Z, Zhao D and Wu S (2014); Linear friction welding of Ti-5Al-2Sn-2Zr-4Mo-4Cr alloy with dissimilar microstructure. J Mater Process Technol., 214, pp. 979-987.

[18] Wang X, Li W, Ma T, Yang X and Vairis A (2019); Effect of welding parameters on the microstructure and mechanical properties of linear friction welded Ti-6.5Al-3.5Mo-1.5Zr-0.3Si joints. J Manuf Process., 46, pp. 100-108.

[19] Wang SQ, Ma TJ, Li WY, Wen GD and Chen DL (2017); Microstructure and fatigue properties of linear friction welded TC4 titanium alloy joints. Sci Technol Weld Join., 22(3), pp. 177-181.

[20] Li WY, Ma T, Zhang Y, Xu Q, Li J and Yang S (2008); Microstructure characterization and mechanical properties of linear friction welded Ti-6Al-4V alloy. Adv Eng Mater., 10, pp. 89-92.

[21] Wang XY, Li WY, Ma TJ and Vairis A (2017); Characterisation studies of linear friction welded titanium joints. Mater Des., 116, pp. 115-126.

[22] Baeslack WA, Broderick TF, Juhas M and Fraser HL (1994); Characterization of solid-phase welds between Ti6A12Sn4Zr2Mo0.1Si and Ti13.5A121.5Nb titanium aluminide. Mater Charact. 15, pp.251-259.

[23] He D, Zhu J, Zaefferer S and Raabe D (2014); Effect of retained beta layer on slip transmission in Ti-6Al-2Zr-1Mo-1V near alpha titanium alloy during tensile deformation at room temperature. Mater Des., 56, pp. 937-942.

[24] Li W, Vairis A, Preuss M and Ma T (2016); Linear and rotary friction welding review. Int Mater Rev., 61(2), pp. 71-100.

[25] Fonda RW, Knipling KE and Bingert JF (2008); Microstructural evolution ahead of the tool in aluminum friction stir welds. Scr Mater., 58, pp. 343-348.